



Performance Analysis of Novel Multi-band Monopole Antenna for Various Broadband Wireless Applications

Hiwa Taha Sediq¹ · Yasser Nozad Mohammed¹

Published online: 21 January 2020
© The Author(s) 2020

Abstract

This study investigates a novel concept of using slot and Coplanar Waveguide fed antenna to obtain multiband operation. The compact antenna includes a star monopole patch with a slit gap and a Star-shape slot on the patch as the radiating part and Dual Square shaped slots on the material as the ground plane. The presentation of techniques in the star-shaped patch and ground plane expands the total length of the current path. This increasing makes the multiband antenna to operate at 4.9 (WLAN), 5.9 (upper WiMAX), 8.2 (satellite TV), 11.8 (X-band) and 17.7 GHz (Ku-band), respectively. The antenna has a physical dimension of $0.32\lambda_0 \times 0.24\lambda_0 \times 0.01\lambda_0 = (20 \times 15 \times 1) \text{ mm}^3$, at the minimum frequency of 4.9 GHz. The proposed configuration operates at 4.9, 5.9, 8.2, 11.8 and 17.7 GHz with bandwidth ($S_{11} < -10 \text{ dB}$) of about 90%, 74.7%, 53.8%, 8.4% and 4.7%, respectively for simulation part. The antenna exhibits measured bandwidth ($S_{11} < -10 \text{ dB}$) of about 108%, 84%, 64%, 9%, and 7% at resonant frequencies of 4.69, 6.03, 7.99, 11.88, and 17.53 GHz, respectively. The stability of the radiation features, $VSWR < 1.5$ and good agreement impedance are noticed across the operating bandwidth of the multiband antenna.

Keywords Star-shaped patch · Gain · Multiband · Reflection coefficient · CPW fed antenna · Radiation pattern

1 Introduction

Nowadays, there are many demands for the new generation of wireless communication systems such as multi-frequency antennas, wide broadband antennas, and small size antennas for mobile and satellite communication systems. Therefore, multi-band antennas consist of various band frequencies that can be applied for more than applications of wireless communication like radar, mobile, and satellite communications [1]. Multi broadband wireless antennas are usually designed by adding fractals [2], multi-split strips, feeding methods [3–6], print slots [7–9], etc. These technologies face some critical points for instance low gain, narrow bandwidth and less efficiency characteristics. However, many researchers attempt to control

✉ Hiwa Taha Sediq
hiwa_eece@yahoo.com

¹ Department of Information Technology, Erbil Polytechnic University, Erbil, Iraq

and resolve their parameters by creating some modifications like multi dielectric methods, slot cut and using different shapes [10, 11].

The main aim of this work designs a small size antenna with multiband frequencies for various applications. Therefore, the technique of slots has been used to design the multiband antenna. Since, slot methods make some discontinuities in the path of electric current which lead to adding extra band frequencies. As a result, a multiple operating frequency is achieved with the aid of various slots [12, 13]. The features of using slots make the antenna more eligible for mobile and wireless devices. The proposed antenna is compared with designs of many researchers who are recently working on multiband wireless devices and different sorts of the antennas examined in writing [14–23], in terms of the size, operational frequencies, bandwidth achieved, gain, and number of operational bands, as represented in Table 1.

A designed low profile monopole antenna works for multi devices like; super WiMAX, wireless computer networks, satellite communication, radar, and Ku-band devices. The overall obtained results of the fabricated and simulated design are in good matching. The proposed planar configuration has small size, multi resonating bands, wide bandwidth, good gain and stable radiation pattern for wireless technologies as compared with those examined in writing [14–23]. In Sect. 2, the design of the monopole antenna and the different steps of the iteration process have been mentioned in detail to achieve the proposed antenna.

2 Antenna Design

2.1 Antenna Geometry

The star patch design is combined from the iteration of the triangle patch shape. Therefore, the equations below have been applied to compute the resonant frequency of this star monopole antenna [24], where S_1 is the length of the triangle side in (mm) as revealed in Fig. 1. All major dimensional parameters of the novel structure are listed in Table 2.

As demonstrated from Fig. 2, the dimensions of the proposed design are $20 \times 15 \text{ mm}^2$ which is printed on the cheap dielectric substrate (FR4) having thickness (h) of 1 mm with loss tangent (δ) and dielectric constant (ϵ_r) of 0.02 and 4.4 separately. The compact configuration consists of a star patch with slit etched on the center of the radiating patch. A coplanar waveguide (CPW) feeding transmission line (50Ω) is used to excite the compact antenna with a strip line of width 1.8 mm and length 8.3 mm. Several antenna parameters, in particular the antenna reflection characteristics can be controlled by the proper impedance of the feed line [25]. The radiating patch is bordered by a U-shaped line of width 0.1 mm which connects both the ground planes on the substrate material. There is a gap distance of 0.3 mm between both radiating materials. The main idea behind of the adding dual square-shape slots ($1 \times 1 \text{ mm}^2$) on the ground plane, in order to produce a new resonant frequency. The copper material with a thickness of 0.035 has been used to design the patch and ground plane of the antenna. Consequently, a star shaped slot with a radius of 3 mm is designed on the center of the radiating patch.

$$\text{Resonance frequency (fr)} \quad fr = \frac{2c}{3S_{eff}\sqrt{\epsilon_{eff}}} \quad (1)$$

Table 1 Measured evaluation of the novel antenna parameters with several existing designs

References	Size (mm ³)	Operating frequency (GHz)	Bandwidth (%)	Gain(dBi)	No. of operating bands	% size reduction
[14]	50×50×1.6	4.76/5.86/9.2	2/12/18.2	6.35/5.57/3.9	3	92.50
[15]	37.62×37.62×2.6	4.7/6.5/7.7/8.5	3.19/2.07/6.75/14.11	5.45/5.42/7.05/5.64	4	91.85
[16]	46×42×1.6	5.68/9.42	3.52/2.65	2.47/5.58	2	90.30
[17]	43×36×1.57	5.15	3.88	3.45	1	87.66
[18]	38.5×38.5×1.57	5.57/7.17/7.65	1.53/2.73/2.98	4.1/3.95/3.54	3	87.11
[19]	46×26×1.6	5/5.8/6.3	8/0.6/0.6	1/0.8/0.6	3	84.32
[20]	34×34×1.6	4/5.5/7/9	47.5/80/62.22	3.39/-4.32/4.39/3.12	4	83.78
[21]	23×26×1.6	4.27/5.57/20	2.11/17.63/3.19	> 2	3	68.65
[22]	20×17.2×1.6	8.95/11.06/11.85	5.02/9.13/3.79	4.45/3.99/4.17	3	45.49
[23]	25×25×0.8	5.2	4.65	5.8	1	40.00
P*	20×15×1	4.69/6.03/7.99/11.88/17.53	108.31/84.24/63.57/8.50/6.84	1.95/2.54/3.57/4.48/5.24	5	—

P* is the proposed work

Fig. 1 **a** Basic structure of triangular patch and **b** first iteration of the triangular patch

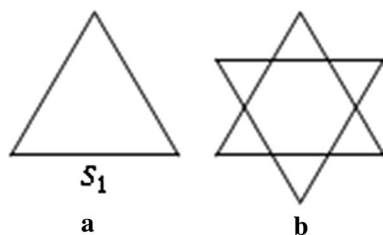
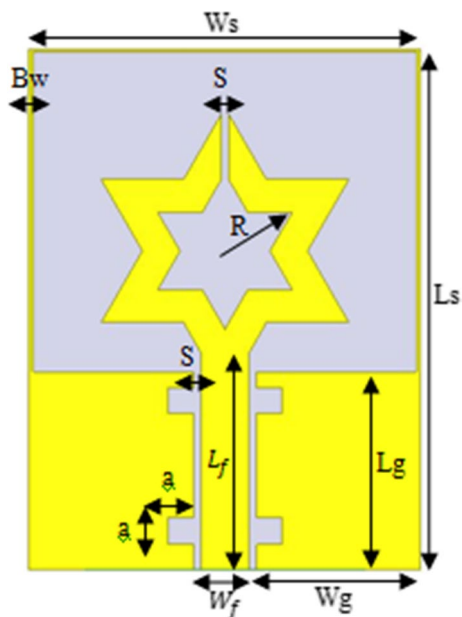


Table 2 Optimized parameters of the prototype antenna

Parameters	Ls	Ws	S	Bw	R
Dimensions (mm)	20	15	0.3	0.1	3
Parameters	Lf	Wf	Lg	Wg	a
Dimensions (mm)	8.3	1.8	7.6	6.3	1

Fig. 2 Geometry of the compact antenna



$$\text{Effective relative Permittivity } (\epsilon_{eff}) \quad \epsilon_{eff} = \frac{\epsilon_r + 1}{2} + \frac{\epsilon_r - 1}{4} \left[1 + 12 \frac{h}{S_1} \right]^{-1/2} \quad (2)$$

$$\text{Effective side length of the triangle } (S_{eff}) \quad S_{eff} = S_1 + \frac{h}{\sqrt{\epsilon_{eff}}} \quad (3)$$

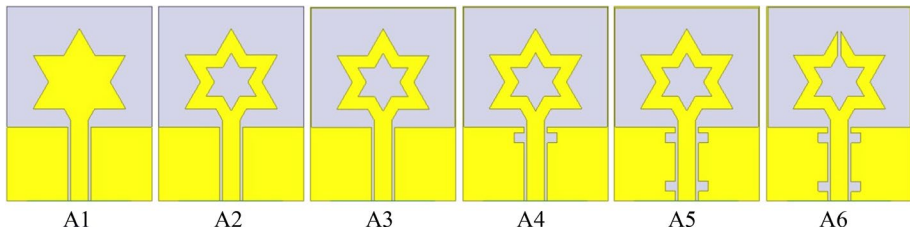


Fig. 3 Configuration of the novel evaluated antenna stages

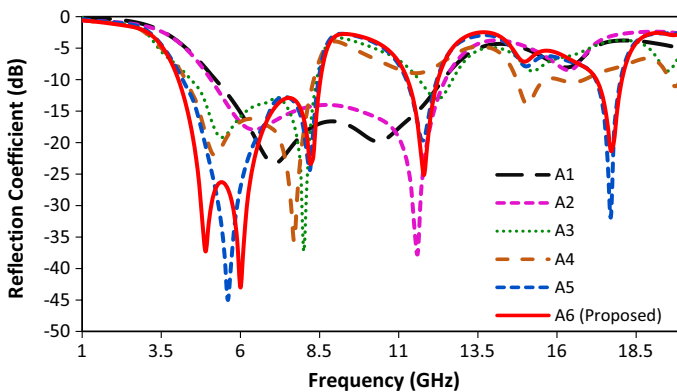


Fig. 4 Evaluation of simulated reflection coefficient (S_{11}) of the antennas

2.2 Design Stages of Proposed Antenna

From Fig. 3, the design stages of the novel five-band antenna are depicted and described step by steps. First of all, a star monopole antenna with the slot method is created as illustrated in the design “A1” of Fig. 3. As can be observed in Fig. 4, this antenna operates only at two bands with less value of reflection parameter S_{11} . A slot star is etched on the radiating patch to improve the parameters of the antenna “A1”, as indicated in configuration “A2” of Fig. 3. So that, the antenna “A2” operates at extra bands, the U-shaped copper material is printed on the border of star monopole as presented in configuration “A3” of Fig. 4. The introduction of U-shaped material leads the antenna to resonate at 11.8 GHz for wireless computer networks and International Telecommunication Union (ITU) band, as revealed in Fig. 4. To insert another operating band for the antenna “A3”, dual square shaped slots are designed on the ground conductive surface of the star monopole structure as demonstrated in configuration “A4” and “A5” of Fig. 3. The effects of the dual square shaped slots make the antenna to operate at 17.7 GHz (Ku-band), as revealed in Fig. 4.

A strip-shaped slot is etched on the top star monopole to further increase the operating skills of antenna “A5”, as indicated in configuration “A6” of Fig. 4. A discontinuity in the radiating element of the monopole antenna is created due to the proposal of strip shaped slot. Because of the discontinuity, the long path of the surface electrical current rises [26]. This increase in the length of current path impacts the input impedance of the star monopole. As a result of this effect, the antenna adds extra resonant frequency at 4.9 GHz for a

wide collection of wireless broadband applications, as indicated in Fig. 4. The design of the novel monopole antenna “A6” is illustrated in detail in the figure of the antenna geometry part as mentioned in advance.

3 Antenna Parametric Studies

The effect of parametric analysis of the antenna is observed to investigate the operation bands of the monopole antenna with the variant of the physical dimension. The optimised parametric study is fulfilled in two circumstances which are (1) variation in U-shaped material width (Bw) of the antenna border, and (2) variation of the width (s) of the strip shaped slot.

For the first condition, all these studies are fulfilled by changing Bw with remaining other parametric dimensions constant as indicated in Fig. 5. The Bw value is changed from 0.1 to 0.4 mm with step of 0.1 mm as depicted from Fig. 5a. As a result of changing the BW value, the reflection coefficient of all bands enhances, bands 1 divides into two bands

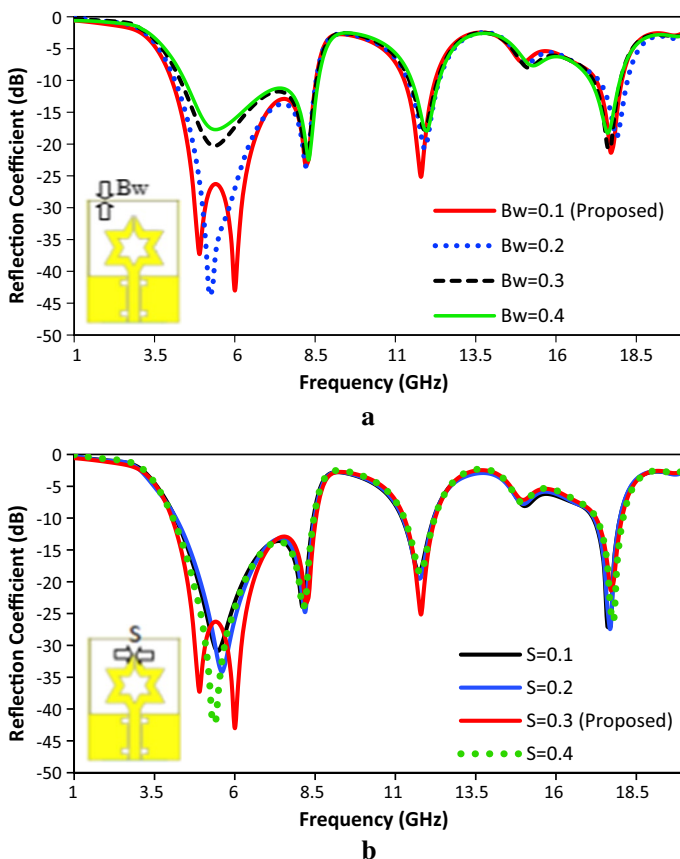


Fig. 5 Parametric analyzes for **a** Bw and **b** S variations

and there exists a slight shift of frequency at whole bands, respectively. The optimum performed results are obtained to the proposed antenna at $Bw=0.1$ mm.

Finally for the second condition, the split gap (S) width observes on the star patch of the compact design. The effects of S width on the parameters of the proposed design are presented where its value is also varied from 0.1 to 0.4 mm. The study reveals that, varied slot width S changes the first band into two bands. As shown from Fig. 5b, the return loss value at bands 1, 2, and 3 enhances. In addition, the S_{11} shifts at band 1 for all S values and its magnitude slightly changes for band 3 and 5. The optimum result is achieved at $S=0.3$ mm for the monopole configuration.

4 Result and Discussion

The novel multiband antenna has been analyzed with assistance of electromagnetic simulator software of High-Frequency Structure Simulator HFSS v.15.0 as depicted in Fig. 2. The monopole antenna depicted in Fig. 6 is fabricated using the same optimized size of the simulated design. The compact dimension of the monopole antenna is $0.32\lambda_0 \times 0.24\lambda_0 \times 0.01\lambda_0$ (20 mm \times 15 mm \times 1 mm), at the minimum resonance of 4.9 GHz.

4.1 Return Loss (S_{11})

The result of the theoretical S_{11} of the design is obtained using Ansoft HFSS and CST software. The electronic device of (VNA) Vector Network Analyzer (N9918A) is used to measure this simulated S_{11} . This study shows that the antenna resonates at 4.9 (WLAN (802.11j)), 5.9 (upper WiMAX), 8.2 (Satellite TV), 11.8 (X-band), and 17.7 GHz (Ku-band) under simulation and at 4.69, 6.03, 7.99, 11.88, and 17.53 GHz in measurement testing, respectively. The simulated bandwidth S_{11} less than -10 dB of the prototype model is about 4.41 GHz (4.1–8.51 GHz), 0.99 GHz (11.27–12.26 GHz), and 0.84 GHz (17.26–18.1 GHz), and about 5.08 GHz (3.56–8.64 GHz), 1.01 GHz (11.45–12.46 GHz), and 1.2 GHz (17.18–18.38 GHz) in measurement, respectively.

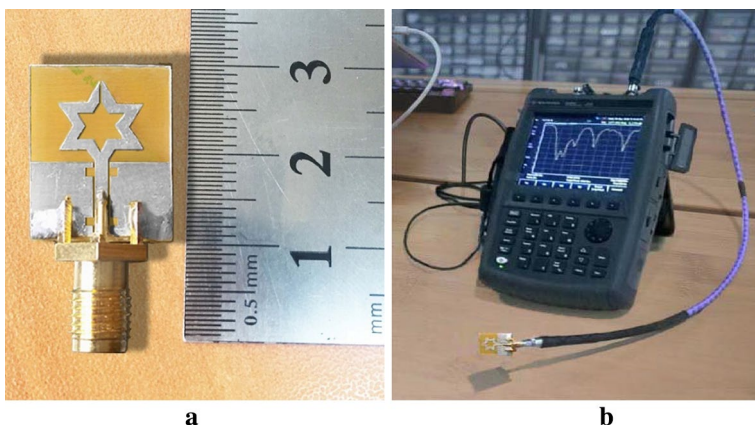


Fig. 6 **a** Fabricated design, and **b** experimental setup of multiband antenna

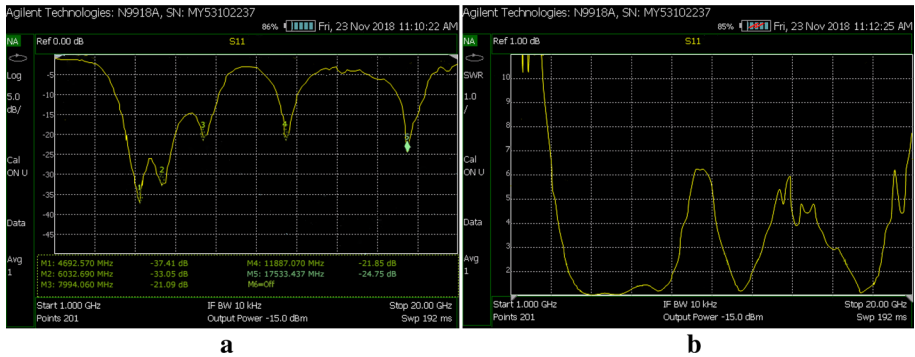


Fig. 7 Experimental view of **a** return loss and **b** VSWR of monopole antenna

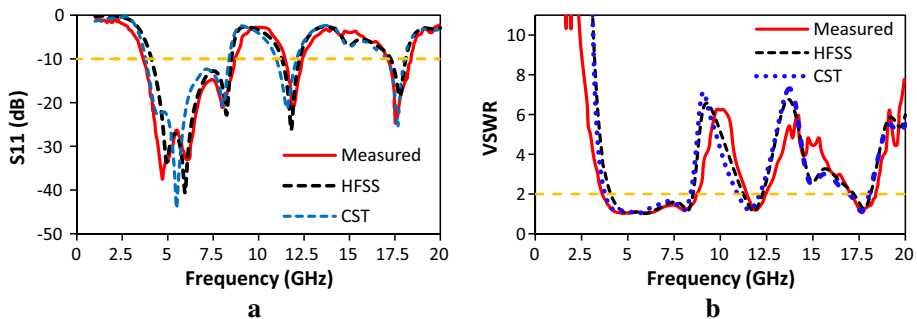


Fig. 8 Comparison results of measured and simulated **a** reflection coefficient and **b** VSWR plots

4.2 Voltage Standing Wave Ratio (VSWR)

In addition, the simulated values of the VSWR is achieved which is about 1.04, 1.01, 1.15, 1.10 and 1.26 at 4.9, 5.9, 8.2, 11.8 and 17.7 GHz, and about 1.02, 1.04, 1.19, 1.19 and 1.12 at 4.69, 6.03, 7.99, 11.88, and 17.53 GHz in the measured values, respectively. The screenshots of the VSWR and the return loss of the fabricated multiband monopole antenna are measured using analyzers as appeared in Fig. 7.

The comparison between the obtained studies of the measurement and simulation of S_{11} and VSWR parameters of the novel antenna is further demonstrated in Fig. 8. A good matching in the obtained results of the theory and experiment is observed for the proposed design. The slight difference may be because of the use of the VNA cable, fabrication tolerance, and point connection of SMA connector and cables applied for the measurement of the configuration. However, the obtained bandwidth of the novel design is enough to fulfill the necessities of WLAN, WiMAX, Satellite communication, ITU-band, and Ku-band applications.

4.3 Surface Current Distribution

The results of surface current distribution was also simulated in HFSS at all resonant frequencies of the proposed multiband antenna as illustrated in Fig. 9 respectively. From the figure has been revealed that current is uniformly distributed on the radiating patch and ground planes at all the resonance bands of the proposed antenna. The surface current has a maximum value at resonant frequency of 11.8 GHz and a minimum magnitude at resonance band of 5.9 GHz for the antenna loaded with U-shape material.

4.4 Radiation Patterns and Gain

Theoretical and experimental far-field radiation characteristics of the monopole star-shape patch antenna are illustrated in Fig. 10. The radiation pattern of the fabricated prototype model is measured from 0 to 360 degree with step of 30 degree, at the resonance bands 4.69, 6.03, 7.99, 11.88, and 17.53 GHz, both in E-plane (co and cross) and H-plane (co and cross), respectively. As can be clearly revealed from Fig. 10, the proposed design has an almost omnidirectional pattern in E-plane (Y–Z) and bi-directional pattern in H-plane (X–Z). For both the cases, the achieved results of the measurement and simulation are in close agreement with a slight deviation because of alignment errors, measurement, and electromagnetic interference from the nearby devices.

The experimental and simulated peak gain along the operational frequencies for the compact structure has been depicted in Fig. 10. The figure shows that fluctuated gain along the desired bands is obtained. The simulated results of achieved gain of each operating frequency at 4.9, 5.9, 8.2, 11.8 and 17.7 GHz are about 1.8, 2.4, 3.6, 4.7 and 4.9 dBi, and

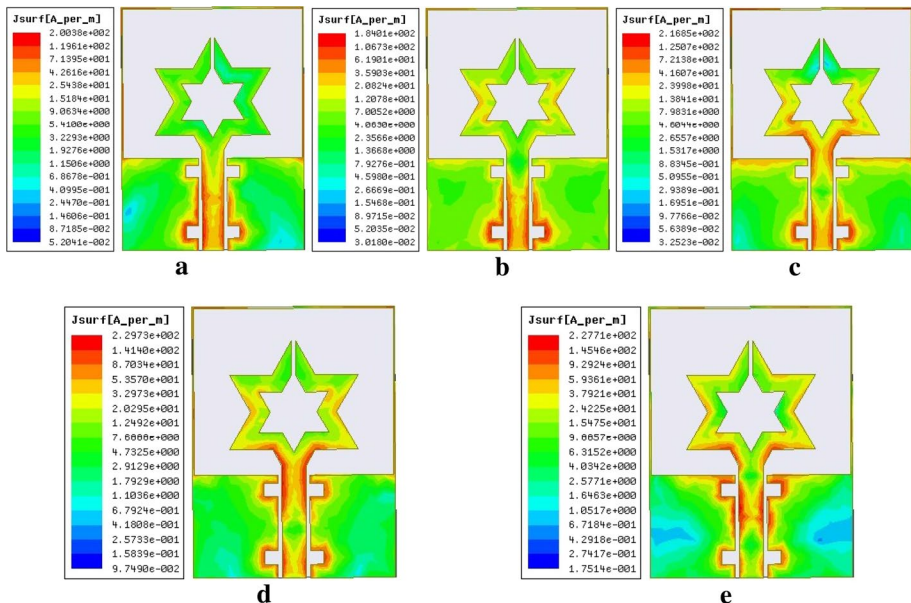


Fig. 9 Surface current distribution of the antenna at **a** 4.9 GHz, **b** 5.9 GHz, **c** 8.2 GHz, **d** 11.8 GHz, **e** 17.7 GHz frequency bands

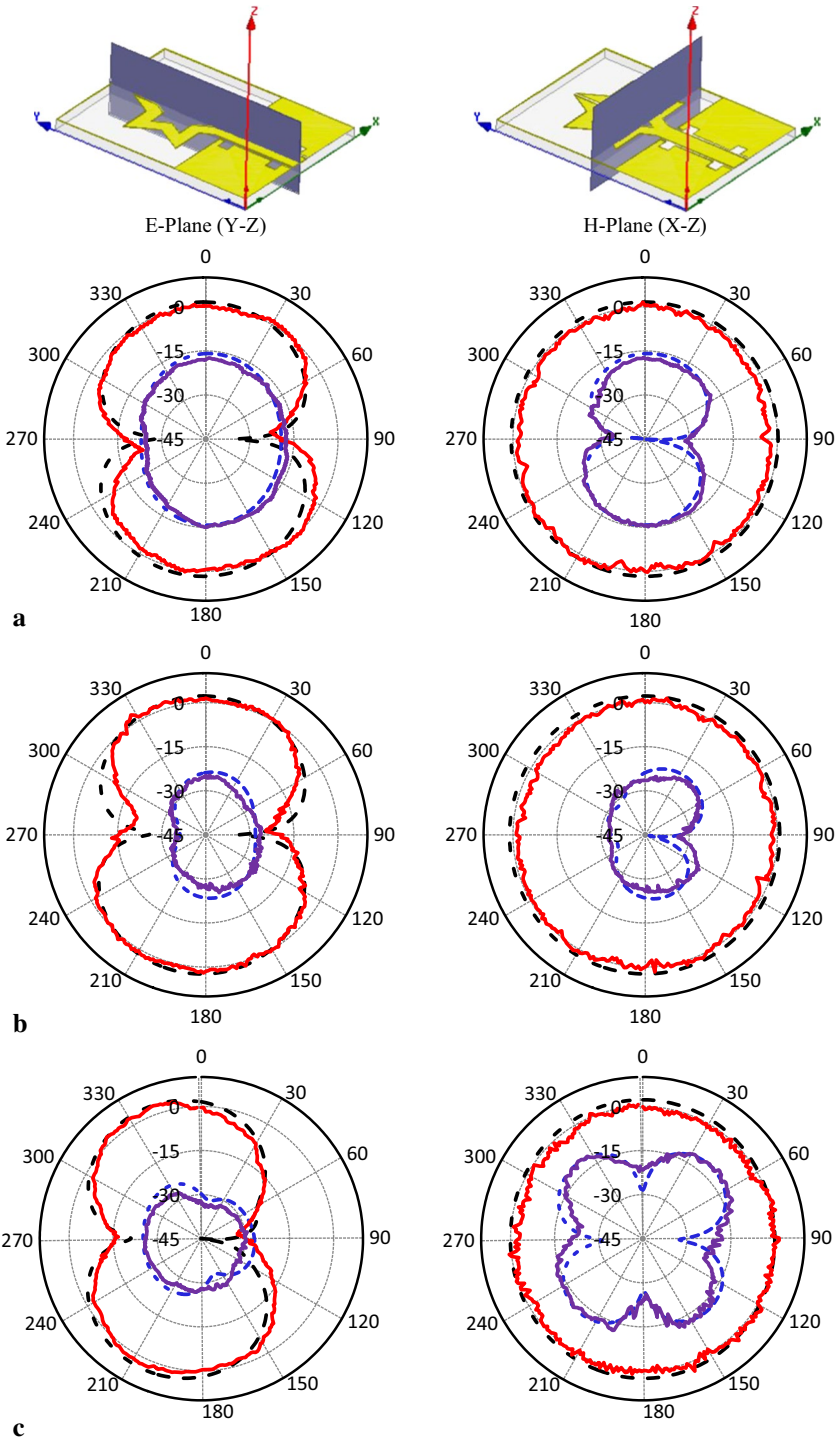


Fig. 10 Measured and simulated radiation characteristics for the evaluated work at **a** 4.69 GHz, **b** 6.03 GHz, **c** 7.99 GHz, **d** 11.88 GHz and **e** 17.53 GHz frequencies

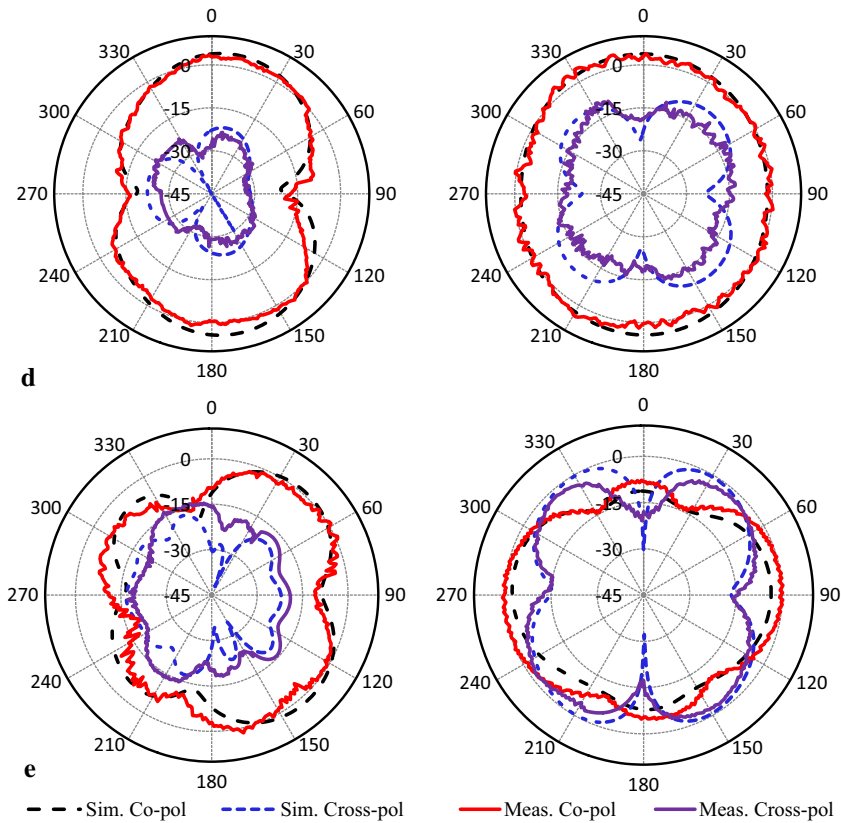


Fig. 10 (continued)

the measured peak gain of approximately 1.95, 2.55, 3.56, 4.48, and 5.24 dBi are observed for 4.69, 6.03, 7.99, 11.88, and 17.53 GHz, respectively. As the results, the average gain of the simulated and measured results is about 3.51 and 3.56 dBi, respectively. The gain value enhances with operational resonances because of the raised effective area of the designed prototype model at shorter wavelengths.

The HFSS software has been used to find the radiation efficiency characteristics of the multiband antenna. The operating band efficiencies are about 94, 94, 84, 87 and 77% at the simulated operating bands of 4.9, 5.9, 8.2, 11.8 and 17.7 GHz, respectively. The star monopole antenna acts as a transmission line instead of radiating part at higher frequencies. Therefore, the magnitude of radiation efficiency decreases at higher resonances as revealed in simulations and Fig. 11. The summarization of the antenna results is listed in Table 3.

5 Conclusion

A compact multiband monopole antenna design loaded with the star-shape slot is studied and with the dimensions of $(20 \times 15 \times 1)$ mm³. The planar design provides the percent bandwidth and the tuning range of about 108% (3.56–8.64 GHz), 84% (3.56–8.64 GHz),

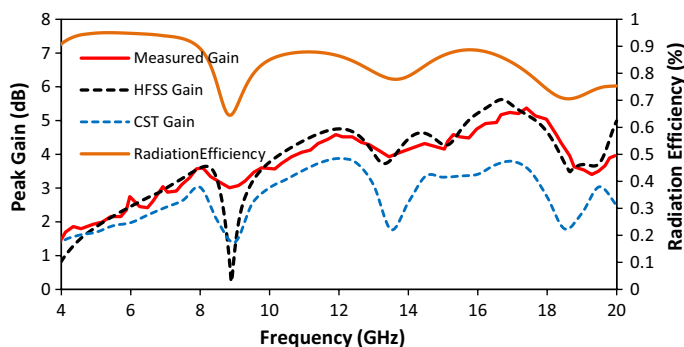


Fig. 11 Results of Gain and efficiency of the multiband antenna

Table 3 Summarization of the multiband antenna results

Frequency band (B)	B1	B2	B3	B4	B5
Operational frequency (GHz)					
Sim.	4.9	5.9	8.25	11.8	17.7
Meas.	4.69	6.03	7.99	11.88	17.53
Peak Gain (dB)					
Sim.	1.81	2.42	3.63	4.73	4.93
Meas.	1.95	2.54	3.57	4.48	5.24
S_{11} (dB)					
Sim.	-33.66	-40.68	-22.76	-26.29	-18.63
Meas.	-37.41	-33.05	-21.09	-21.09	-24.75
VSWR					
Sim.	1.04	1.01	1.15	1.10	1.26
Meas.	1.02	1.04	1.19	1.19	1.12
Tuning range (GHz)					
Sim.	4.1–8.51	4.1–8.51	4.1–8.51	11.27–12.26	17.26–18.1
Meas.	3.56–8.64	3.56–8.64	3.56–8.64	11.45–12.46	17.18–18.38
Bandwidth (%)					
Sim.	90	74.75	53.78	8.39	4.75
Meas.	108.31	84.24	63.57	8.50	6.84
Applications					
	WLAN	WiMAX	Satellite TV	X-band	Ku-band

64% (3.56–8.64 GHz), 9% (11.45–12.46 GHz), and 7% (17.18–18.38 GHz), at the various measured operational bands. The analyses of the parametric antenna reveal that the slight modifying in the optimised dimensional antenna influence the surface current distribution, which leads to increase the number of the frequency bands of the proposed technology.

Simulation and measurement parts are applied to investigate the results of the compact antenna with respect to the antenna parameters of S_{11} , gain, VSWR, and radiation pattern. The experimental results reveal that the novel planar antenna has five frequencies at about 4.69, 6.03, 7.99, 11.88, and 17.53 GHz, with stable radiation characteristics, VSWR < 1.5 and good matching impedance. Due to the mentioned purpose, the proposed design can

easily be a good candidate for WLAN, WiMAX, Satellite communications, X-band, and Ku-band applications.

Acknowledgement The author thank of the University of Birmingham in the UK for fabricating the antennas and Erbil Polytechnic University for supporting this study.

Open Access This article is licensed under a Creative Commons Attribution 4.0 International License, which permits use, sharing, adaptation, distribution and reproduction in any medium or format, as long as you give appropriate credit to the original author(s) and the source, provide a link to the Creative Commons licence, and indicate if changes were made. The images or other third party material in this article are included in the article's Creative Commons licence, unless indicated otherwise in a credit line to the material. If material is not included in the article's Creative Commons licence and your intended use is not permitted by statutory regulation or exceeds the permitted use, you will need to obtain permission directly from the copyright holder. To view a copy of this licence, visit <http://creativecommons.org/licenses/by/4.0/>.

References

1. Choukiker, Y. K., Behera, S. K., Pandey, B. K., & Jyoti, R. (2010). Optimization of planar antenna for ISM band using PSO. In *Second international conference on computing communication and networking technologies (ICCCNT)*, Karur (pp. 1–4). IEEE.
2. Anguera, J., Puente, C., Borja, C., & Soler, J. (2005). Fractal shaped antennas: A review. *Encyclopedia of RF and Microwave Engineering*. <https://doi.org/10.1002/0471654507.emc128>.
3. Sarkar, D., Saurav, K., & Srivastava, K. V. (2014). Multi-band microstrip-fed slot antenna loaded with split-ring resonator. *Electronics Letters*, 50(21), 1498–1500.
4. Elsheakh, D. M., Elsadek, H. A., Abdallah, E. A., Iskander, M. F., & El-Hennawy, H. M. (2010). Reconfigurable single and multiband inset feed microstrip patch antenna for wireless communication devices. *Progress in Electromagnetics Research*, 12, 191–201.
5. Bakariya, P. S., Dwari, S., Sarkar, M., & Mandal, M. K. (2015). Proximity-coupled microstrip antenna for bluetooth, WiMAX, and WLAN applications. *IEEE Antennas and Wireless Propagation Letters*, 14, 755–758.
6. Wu, R. Z., Wang, P., Zheng, Q., & Li, R. P. (2015). Compact CPW-fed triple-band antenna for diversity applications. *Electronics Letters*, 51(10), 735–736.
7. Mehdi pour, A., Sebak, A. R., Trueman, C. W., & Denidni, T. A. (2012). Compact multiband planar antenna for 2.4/3.5/5.2/5.8-GHz wireless applications. *IEEE Antennas and Wireless Propagation Letters*, 11, 144–147.
8. Wang, H., & Zheng, M. (2011). An internal triple-band WLAN antenna. *IEEE Antennas and Wireless Propagation Letters*, 10, 569–572.
9. Ali, T., Khaleeq, M. M., Pathan, S., & Biradar, R. C. (2018). A multiband antenna loaded with meta-material and slots for GPS/WLAN/WiMAX applications. *Microwave and Optical Technology Letters*, 60(1), 79–85.
10. Sediq, H. T. (2018). Design of ultra-wideband dipole antenna for WiMAX wireless applications. *Polytechnic Journal*, 8(3), 13–25.
11. Salamin, M. A., Das, S., & Zugari, A. (2018). Design and realization of low profile dual-wideband monopole antenna incorporating a novel ohm (Ω) shaped DMS and semi-circular DGS for wireless applications. *AEU-International Journal of Electronics and Communications*, 97, 45–53.
12. Lee, S. H., Lim, Y., Yoon, J. J., Hong, C. B., & Kim, H. I. (2010). Multiband folded slot antenna with reduced hand effect for handsets. *IEEE Antennas and Wireless Propagation Letters*, 9, 674–677.
13. Yuan, B., Cao, Y., & Wang, G. (2011). A miniaturized printed slot antenna for six-band operation of mobile handsets. *IEEE Antennas and Wireless Propagation Letters*, 10, 854–857.
14. Vinodha, E., & Raghavan, S. (2017). Double stub microstrip fed two elements Rectangular Dielectric Resonator Antenna for multiband operation. *AEU-International Journal of Electronics and Communications*, 78, 46–53.
15. Kohli, S., Dhillon, S. S., & Marwaha, A. (2013). Design and optimization of multiband fractal microstrip patch antenna for wireless applications. In: *5th International Conference on Computational Intelligence and Communication Networks* (pp. 32–36). IEEE.

16. Kaushal, D., Shanmuganatham, T., & Sajith, K. (2017). Dual band characteristics in a microstrip rectangular patch antenna using novel slotting technique. In *2017 International conference on intelligent computing, instrumentation and control technologies (ICICICT)* (pp. 957–960). IEEE.
17. Alqadami, A. S., Jamlos, M. F., Soh, P. J., Rahim, S. K., & Narbudowicz, A. (2017). Left-handed compact MIMO antenna array based on wire spiral resonator for 5-GHz wireless applications. *Applied Physics A*, 64(1), 123–127.
18. Kumar, A., & Raghavan, S. (2018). Design of SIW cavity-backed self-triplexing antenna. *Electronics Letters*, 54(10), 611–612.
19. Ibrahim, A. A., Abdalla, M. A., & Hu, Z. (2018). Compact ACS-fed CRLH MIMO antenna for wireless applications. *IET Microwaves, Antennas and Propagation*, 12(6), 1021–1025.
20. Choukiker, Y. K., & Behera, S. K. (2014). Modified Sierpinski square fractal antenna covering ultra-wide band application with band notch characteristics. *IET Microwaves, Antennas and Propagation*, 8(7), 506–512.
21. Pandeewari, R. (2018). Complimentary split ring resonator inspired meandered CPW-fed monopole antenna for multiband operation. *Progress in Electromagnetics Research*, 80, 13–20.
22. Samsuzzaman, M., & Islam, M. T. (2014). Inverted S-shaped compact antenna for X-band applications. *The Scientific World Journal*. Article ID 604375.
23. Hu, J. R., & Li, J. S. (2014). Compact microstrip antennas using CSRR structure ground plane. *Micro-wave and Optical Technology Letters*, 56(1), 117–120.
24. Marzudi, W., Najwa, W. N., Zainal Abidin, Z., Dahlan, S. H., Ramli, K. N., & Kamarudin, M. R. (2015). Performance of Star patch antenna on a paper substrate material. *ARPJ Journal of Engineering and Applied Sciences*, 10(19), 8606–8612.
25. Hu, Y., Jackson, D. R., Williams, J. T., Long, S. A., & Komanduri, V. R. (2008). Characterization of the input impedance of the inset-fed rectangular microstrip antenna. *IEEE Transactions on Antennas and Propagation*, 56(10), 3314–3318.
26. Ali, T., Saadh, A. M., Biradar, R. C., Anguera, J., & Andújar, A. (2017). A miniaturized metamaterial slot antenna for wireless applications. *AEU-International Journal of Electronics and Communications*, 82, 368–382.

Publisher's Note Springer Nature remains neutral with regard to jurisdictional claims in published maps and institutional affiliations.



Hiwa Taha Sediq was born on 23 of June 1981 in a small town (Shaqalawa) where belongs to the capital city of Kurdistan in Iraq. He was awarded Bachelor's degree in Physics in 2005 from the University of Salahadden in Erbil. After his graduation, he was working for computer department as a teacher for 5 years and in charge of internet unit for 2 years in Shaqlawa Technical Institute and he is also head of information technology department at the same institute. He received the M.Sc. degree in Communication Engineering from University of Birmingham in Unite Kingdom in 2013. His prime research interest is in the areas of wireless communications with focus on antenna applications.



Yasser Nozad Mohammed was born in 1984 in a small town in Iraq. He was awarded Bachelor's degree in computer in 2007 from the University of Alyarmouk in Iraq. After his graduation, he was working for computer department as a teacher for 11 years. He received the M.Sc. degree in Computer Engineering from European University of Lefke in Cyprus in 2015. His research interest is in the areas of wireless communications and Networks.